Magnetic Impurities on the Surface of a Topological Insulator

Qin Liu,[1] Chao-Xing Liu,[2,3] Cenke Xu,[4] Xiao-Liang Qi,[3] and Shou-Cheng Zhang[3]
[1]*Department of Physics, Fudan University, Shanghai 200433, China*
[2]*Center for Advanced Study, Tsinghua University, Beijing, 100084, China*
[3]*Department of Physics, McCullough Building, Stanford University, Stanford, California 94305-4045, USA*
[4]*Department of Physics, Harvard University, Cambridge, Massachusetts 02138, USA*
(Received 21 August 2008; published 17 April 2009)

The surface states of a topological insulator are described by an emergent relativistic massless Dirac equation in 2 + 1 dimensions. In contrast with graphene, there is an odd number of Dirac points, and the electron spin is directly coupled to the momentum. We show that a magnetic impurity opens up a local gap and suppresses the local density of states. Furthermore, the Dirac electronic states mediate an RKKY interaction among the magnetic impurities which is always ferromagnetic, whenever the chemical potential lies near the Dirac point. Through this exchange mechanism, magnetic atoms uniformly deposited on the surface of a topological insulator could naturally form a ferromagnetically ordered film. These effects can be directly measured in STM experiments. We also study the case of quenched disorder through a renormalization group analysis.

DOI: 10.1103/PhysRevLett.102.156603 PACS numbers: 72.25.Dc, 73.20.−r, 75.30.Hx, 85.75.−d

Following the recent theoretical prediction and the experimental observation of the quantum spin Hall insulator state in two dimensions [1–4], the concept of a topological insulator (TI) in three dimensions has attracted a lot of interest [5–8]. The electronic excitation spectrum of a time reversal (TR) invariant TI is fully gapped in the bulk, but there are gapless surface states described by the (2 + 1)-dimensional [(2 + 1)D] relativistic Dirac equation with an odd number of Dirac points. This property makes the surface system an extremely unusual (2 + 1)D system, just like the (1 + 1)D "helical" edge states of quantum spin Hall insulators [9,10]. In fact, one can prove a general no-go theorem, which states that a two-dimensional TR invariant lattice model cannot have an odd number of Dirac points [9]. For example, the familiar graphene model on a honeycomb lattice has four Dirac points [11,12]. The surface states of a TI evade this no-go theorem since they describe the boundary of a three-dimensional lattice model, and a pair of Dirac points can be separated onto the two opposite surfaces. The Dirac points of a TI are thus stable and robust. They can not be destroyed by any TR invariant perturbations. In contrast, since the Dirac points of a two-dimensional lattice model occur in pairs, they can be pairwise annihilated by small perturbations. For example, a sublattice distortion in graphene can remove Dirac points entirely.

Therefore, the surface states of a TI offer a unique platform to investigate the physics of robust Dirac points. In Refs. [8,13], it was pointed out that a TR breaking perturbation on the surface is the most natural way to reveal the topological properties of Dirac points. For this reason, we investigate the effects of magnetic impurities on the surface states of a TI. We consider the simplest case of a single Dirac point, described by the low-energy effective Hamiltonian

$$\hat{H}_0 = \sum_{k,\alpha,\beta} \psi^\dagger_{k\alpha} h_{\alpha\beta}(\mathbf{k}) \psi_{k\beta},$$
$$h_{\alpha\beta}(k) = \hbar v_f (k_x \sigma^x_{\alpha\beta} + k_y \sigma^y_{\alpha\beta}), \tag{1}$$

where the z direction is perpendicular to the surface and v_f is the Fermi velocity. At first sight, this is exactly the 2D Dirac Hamiltonian at one nodal point of graphene which has been used successfully to describe its low-energy physics [11,12]. However, there is one important difference between these two cases. For graphene, the two components of the Dirac Hamiltonian describe the two sublattices or pseudospin degrees of freedom, while in the case of a TI, the two components describe the real electron spin, and are related to each other by TR. Therefore, we expect the coupling between magnetic impurities and electron spin to take the form

$$\hat{H}_{\text{ex}} = \hat{H}^z_{\text{ex}} + \hat{H}^{\parallel}_{\text{ex}} = \sum_r J_z s_z(\mathbf{r}) S_z(\mathbf{r}) + J_{\parallel}(s_x S_x + s_y S_y)(\mathbf{r}), \tag{2}$$

where $S_i(\mathbf{r})$ is the spin of a magnetic impurity located at $\mathbf{r}$, $s_i(\mathbf{r}) = \psi^\dagger(\mathbf{r})\sigma^i\psi(\mathbf{r})$ is the spin of the surface electrons and J_z, $J_\parallel$ are the coupling parameters. The Hamiltonians (1) and (2) together describe the problem of magnetic impurities on the surface of a TI, which is the starting point of this Letter. Recently, Bi_2Se_3, Bi_2Te_3, and Sb_2Te_3 have been predicted to be topological insulators with a single Dirac surface state [14,15]. Taking Sb_2Te_3 as an example, which can be doped with vanadium as magnetic impurities [16,17], the effective surface model (1) can be derived microscopically, with the Fermi velocity $\hbar v_f \approx 3.7\ \text{eV} \cdot \text{Å}$. According to the bulk exchange coupling be-

tween electrons and magnetic impurities [16], the surface exchange parameters J_z and $J_\parallel$ are estimated of order 0.1–0.5 eV, which depends on the overlap between the surface states and the magnetic impurities. Furthermore, the Fermi level lies close to the Dirac point.

Single magnetic impurity.—Let us start by studying the effect of a single magnetic impurity on the surface states. For simplicity, we treat the impurity as a classical spin locating at the origin. Under such a mean-field approximation, the exchange Hamiltonian is written as

$$\hat{H}_{\text{ex}} = \sum_{\mathbf{r}} M_i(\mathbf{r}) s_i(\mathbf{r}), \qquad i = x, y, z. \tag{3}$$

Here we study the case with the impurity spin polarized in the z direction ($M_x = M_y = 0$) and take a square well regularization for the finite range exchange interaction with the form $M_z(\mathbf{r}) = M_0\Theta(r_0 - r)$ where $\Theta(r_0 - r)$ is the step function and $M_0 = J_z\langle S_z\rangle$. r_0 determines the range of the exchange interaction. This problem has azimuthal symmetry and can be solved analytically with Bessel functions [18]. From the analytic solution we find that the wave function for $r < r_0$ decays for energies $|E| < |M_0|$, and oscillates for energies $|E| > |M_0|$. To study observable consequences of this impurity effect, we calculate the local density of states (LDOS) defined by $\rho_0(\mathbf{r}, E) = -\frac{1}{2\pi}\Im\{\mathrm{Tr}[G^R(\mathbf{r}, \mathbf{r}, E)]\}$, where $G^R(\mathbf{r}, \mathbf{r}', E)$ is the retarded single-particle Green's function. As shown in Figs. 1(a) and 1(b), the LDOS is suppressed in the energy range $|E| < |M_0|$ and spatial range $r < r_0$. For $r > r_0$ the LDOS converges quickly to the impurity-free value $\frac{|E|}{2\pi\hbar^2 v_f^2}$. Such a LDOS gap induced by a magnetic impurity can be observed by STM experiments, and define a sharp criterion to distinguish the TI surface from other two-dimensional systems with an even number of Dirac cones, such as graphene. In graphene, the two components of the Dirac Hamiltonian represent the pseudospin degree of freedom of the two sublattices, which do not couple to magnetic impurities directly. Therefore, no suppression of LDOS will be observed [19].

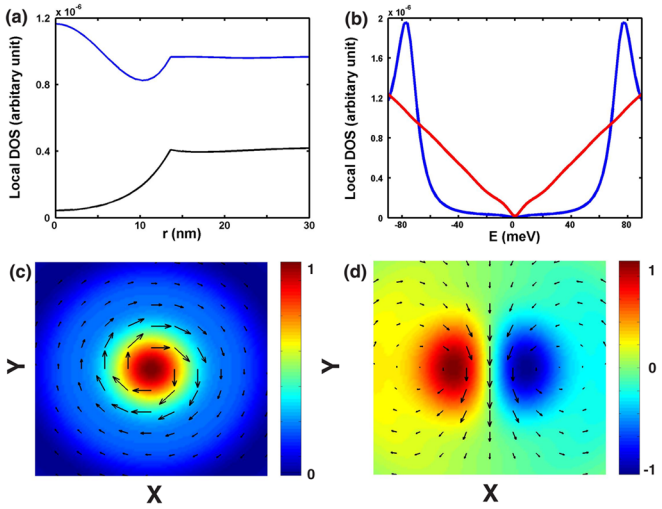

FIG. 1 (color online). (a) Charge local density of states (LDOS) as a function of the distance r from the magnetic impurity for electron energies $E = 30$ meV (black line) and $E = 70$ meV (blue line). (b) Charge LDOS as a function of electron energy E at positions $r = 0$ (blue line) and $r = 20$ nm (red line). Here we assume a magnetic impurity strength $M_0 = 50$ meV and a coupling range $r_0 = 13$ nm. The spin LDOS is plotted as a function of position at $E = 10$ meV for magnetization of the magnetic impurity placed at the origin (0,0) in (c) the z direction and (d) the y direction. Here the arrow indicates the in-plane spin LDOS and the color shows the z direction spin LDOS.

Another interesting physical quantity is the spin LDOS, defined by $\rho_i(\mathbf{r}, E) = -\frac{1}{2\pi}\Im\{\mathrm{Tr}[G^R(\mathbf{r}, \mathbf{r}, E)\sigma_i]\}$, $i = x, y, z$. Experimentally, the spin LDOS can be measured by the recently developed spin-resolved STM technique [20]. Without the azimuthal symmetry in general the system cannot be solved analytically anymore, we then adopt the standard T-matrix formalism [21,22] to calculate the Green's function $G^R(\mathbf{r}, \mathbf{r}', E)$ numerically with the exchange coupling in (3) regarded as a δ function $M_i(\mathbf{r}) = J_i\langle S_i\rangle\delta(\mathbf{r})$. The calculated distribution of the spin LDOS $\rho_i(\mathbf{r}, E)$ at a given energy is shown in Fig. 1(c) for the out-of-plane and (d) for in-plane magnetization, respectively. As seen from Fig. 1(c), the z-direction magnetization induces not only a z-direction spin LDOS, but also an in-plane spin LDOS. This is a direct consequence of the spin-orbit coupling of surface states. In fact, the Dirac Hamiltonian (1) can be regarded as an electron spin coupled to a momentum-dependent effective magnetic field $\mathbf{B}_{\text{eff}} = \hbar v_f \mathbf{k}$. As an electron propagates, its spin processes around $\mathbf{B}_{\text{eff}}$. Since $\mathbf{B}_{\text{eff}}$ is parallel to the propagation direction of the electron, the electron spin always precesses in a plane perpendicular to the direction of propagation. For example, when an electron with spin polarized in the z direction is moving towards the x direction, the spin is precessing in the yz plane. Consequently, the spin LDOS vector $\rho_s(\mathbf{r}, E) = (\rho_x, \rho_y, \rho_z)$ is canted towards the y direction when $\mathbf{r}$ is along the positive x axis. A similar analysis can apply to other directions, from which we can understand the spin LDOS distribution in Fig. 1(c). For an in-plane impurity spin polarized in the y direction shown in Fig. 1(d), the precession picture remains valid. The spin LDOS pattern in Figs. 1(c) and 1(d) can also be understood by symmetry. When the impurity spin is polarized in the z direction, the system is invariant under the rotations about z axis, and so is the spin LDOS. For an in-plane impurity spin, rotation symmetry is broken, but there is a discrete symmetry defined by a π-rotation along the z axis combined with a TR transformation. Such a residual symmetry is preserved in the pattern of Fig. 1(d).

Besides the patterns discussed above which are due to spin precession, another important feature of the spin LDOS is the longitudinal decay $\rho_i \propto 1/r^2$ when Fermi energy is near the Dirac point. After integrating over energies below Fermi energy, the local spin polarization $\langle\mathbf{s}(\mathbf{r})\rangle$ behaves as $1/r^3$. Such a $1/r^3$ power law is a direct

consequence of the fact that the spatial scaling dimension of the spin density in the free Dirac fermion theory is 2.

Random magnetic impurities.—In the following we will focus on the behavior of the system with randomly distributed magnetic impurities on the surface $\mathbf{S}(\mathbf{r}) = \sum_i \mathbf{S}_i \delta(\mathbf{r} - R_i)$, where $\mathbf{R}_i$ are the positions of magnetic impurities. As every magnetic impurity will open a local gap in its vicinity, we may expect the system to be gapped everywhere, at least in the mean-field level. However, this is not necessarily true if the magnetization of magnetic impurities is nonuniform. To see this, we consider again the mean-field form of the exchange Hamiltonian (3) with a magnetization domain wall along the y axis at $x = 0$, which is given by $M_z(x) > 0$ ($M_z(x) < 0$) for $x > 0$ ($x < 0$) and $M_x = M_y = 0$. Solving the Schrödinger equation directly on the domain wall, we obtain gapless chiral fermion modes along the domain wall with wave function $\psi \sim (1, i)^T \times \exp[ik_y y - \int_0^x \frac{M_z(x)}{\hbar v_f} dx]$ and energy dispersion $E = \hbar v_f k_y$. Thus, this system is in fact not totally gapped but has gapless modes. Compared with the fully gapped system, the appearance of such gapless modes will cost more energy. Therefore, heuristically we expect the system not to favor any magnetic domain wall, which indicates that magnetic impurities should be ferromagnetically coupled.

Keeping such a heuristic picture in mind, we now study the coupling between two magnetic impurities microscopically. The itinerant electrons can mediate a spin interaction between two magnetic impurities, known as the Ruderman-Kittel-Kasuya-Yosida (RKKY) interaction. Such a coupling can be obtained by integrating out the fermions in the Hamiltonians (1) and (2), which results in the form $\hat{H}_{\text{in}} = \sum_{i,j=x,y,z} \Phi_{i,j}(|\mathbf{r} - \mathbf{r}'|) S_{1i}(\mathbf{r}) S_{2j}(\mathbf{r}')$ for any two magnetic impurities S_1 and S_2. The coupling constant $\Phi_{ij}(R)$ is a function of $R = |\mathbf{r} - \mathbf{r}'|$ and can be extracted from standard second-order perturbation theory. For example, the z-direction coupling constant has the form $\Phi_{zz}(R) = \frac{J_z^2 a_0^4}{\hbar v_f R^3}(F_+(k_F R) + F_-(k_F R))$, where k_F is the Fermi momentum, a_0 is the lattice constant and $F_{+(-)}(x_F) = \int_0^{x_F(x_c)} \frac{x dx}{2\pi} \int_{x_F}^{x_c} \frac{x' dx'}{2\pi} \frac{1}{+(-)x - x'} [J_0(x) J_0(x') - (+) J_1(x) J_1(x')]$. $J_n(x)$ is the Bessel function and $x_c = k_c R$ with k_c a large momentum cutoff. The oscillating part of the RKKY interaction is determined by $F_+ + F_-$ and the decaying part is proportional to $1/R^3$. Such dependence is related to the $1/r^3$ dependence of the local spin polarization induced by a single magnetic impurity discussed earlier. Being a consequence of the Dirac Hamiltonian, similar behavior has also been found in graphene [23,24]. The novel property of Dirac fermions appears when the chemical potential is close to the Dirac point. Since the oscillation period of the RKKY interaction is determined by Fermi wavelength $\lambda_F = 1/k_F$, the oscillation becomes weaker as $k_F \to 0$, as shown in Fig. 2. Eventually two magnetic impurities become ferromagnetically coupled when λ_F is much larger than the average distance between them.

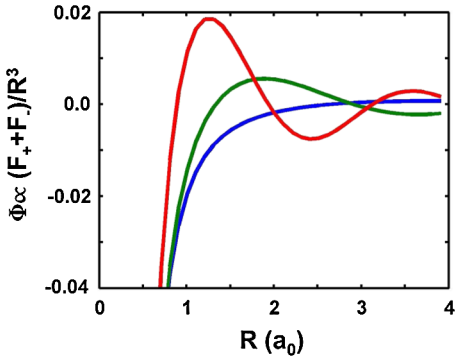

FIG. 2 (color online). RKKY interaction versus the distance R between two magnetic impurities. Fermi momentum k_F is chosen to be $0.5/a_0$ for the blue line, $1.0/a_0$ for the green line and $1.5/a_0$ for the red line, where a_0 is the lattice constant.

Because of the ferromagnetic RKKY interaction discussed above, we expect ferromagnetic order to appear among the magnetic atoms doped on the surface of a TI when the chemical potential is near the Dirac point. At the mean-field level, from the $\hat{H}_{\text{ex}}^z$ term in (2) we know that $J_z \langle s_z \rangle$ acts as an effective magnetic field to magnetize the magnetic impurities. At the same time, $J_z \langle S_z \rangle$ acts as the effective magnetic field to polarize the electron spin. The behavior of the critical temperature T_c for the ferromagnetism can be extracted from a standard calculation [25], and is given by $k_B T_c = \frac{S_0(S_0+1) a_0^2 y}{6\pi\hbar^2 v_f^2} J_z^2 (E_c - E_f)$, where E_c is a cutoff energy, E_f is the Fermi energy, and S_0 is the saturation spin value of each magnetic impurity. Setting $y = 0.2$, $a_0 = 4.25$ Å, $E_c = 0.1$ eV and $S_0 = 1$ for vanadium ions [16], T_c is estimated within the range 0.3–8 K. Interestingly, such a ferromagnetically ordered surface state also carries a half quantized Hall conductance $\sigma_H = \pm e^2/2h$, which can be understood as the parity anomaly of massless Dirac fermions [26,27], and is a direct manifestation of the nontrivial topology of the bulk system.

Quenched magnetic disorder.—We have calculated the spin LDOS distribution around an isolated magnetic impurity, this distribution can be potentially modified by interaction and quenched disorder. It is obvious that for 2D Dirac system, the short range interaction is an irrelevant perturbation, and hence will not affect the long distance spin LDOS distribution. We now consider the effects of quenched disorder on the response to the isolated magnetic impurity. In the current work, we only consider the random XY moment, which couple to the Dirac fermion by the following means: $\mathcal{L}' = -v_f g B_j(\mathbf{r}) \psi^\dagger(\mathbf{r}) \sigma^j \psi(\mathbf{r})$, where $j = x, y$. A more comprehensive analysis of random potentials will be published elsewhere. $B_j(\mathbf{r})$ represents the random potential with correlation $\langle B_i(\mathbf{r}) B_j(\mathbf{r}') \rangle = \delta_{ij} \delta^2(\mathbf{r} - \mathbf{r}')/(2\pi)$. g^2 is proportional to the standard deviation of each component of random potential, which from naive power counting is a marginal perturbation, and hence it may modify the long distance response. Since the random potential has long-range temporal corre-

lation but short-range spatial correlation, Lorentz invariance of the bare Dirac Lagrangian is lost, and the Fermi velocity v_f flows under RG. In the calculation we assume that the standard deviation $\Delta \sim g^2$ is small. After integrating out degrees of freedom between momentum cutoff $\tilde{\Lambda}$ and Λ, the leading order RG equations read

$$\frac{dv_f}{d\ln l} = -\frac{g^2 v_f}{2\pi^2}, \qquad \frac{dZ_\psi}{d\ln l} = -\frac{g^2}{2\pi^2}, \qquad \frac{dZ_{v0}}{d\ln l} = \frac{g^2}{2\pi^2}, \qquad \frac{dZ_{vz}}{d\ln l} = \frac{g^2}{2\pi^2}, \qquad \frac{dZ_{vxy}}{d\ln l} = 0. \tag{4}$$

Z_ψ is the wave function renormalization and Z_{v0}, Z_{vxy}, and Z_{vz} are vertex corrections to $\psi^\dagger\psi$, $\psi^\dagger\sigma^{x(y)}\psi$, and $\psi^\dagger\sigma^z\psi$, respectively. The solution of the RG equations reads $z = 1 + \frac{g^2}{2\pi^2}$, $\Delta[v_f] = \frac{g^2}{2\pi^2}$, $\Delta[\psi^\dagger\psi] = 2$, $\Delta[\psi^\dagger\sigma^z\psi] = 2$, $\Delta[\psi^\dagger\sigma^{x(y)}\psi] = 2 + \frac{g^2}{2\pi^2}$. The dynamical scaling dimension z is changed because the Fermi velocity acquires a nonzero scaling dimension under RG, leading to the following scaling of the LDOS: $\rho(\omega) \sim \omega^{(2-z)/z}$ [28]. With the above scaling dimensions of the fermion bilinears, the long distance spin distribution around an isolated magnetic impurity with in-plane moment is given by $s^{x(y)}(r) = \psi^\dagger\sigma^{x(y)}\psi(r) \sim \frac{1}{r^{3+g^2/\pi^2}}$. Thus the spin polarization pattern remains similar to that shown in Figs. 1(c) and 1(d), but decays with a different power law.

In realistic system, the chemical potential may not locate exactly at the Dirac point, in this case the finite chemical potential becomes an infrared cutoff of our RG calculations, our result above can be applied to the distance shorter than $1/k_f \sim 37$ nm for the typical Fermi energy $\sim$10 meV. Quenched disorder has been studied in graphene, with $N = 4$ flavors of Dirac fermions [29–31]. In this case, ripples of a graphene sheet, interpreted as a random "gauge potential" $B_j(x)\psi^\dagger\sigma^j\psi$, have attracted most of the attention. In contrast with our results, the $1/N$ expansion is usually taken when the RG equations are derived for graphene. The competition between random potentials and the Coulomb interaction has also been studied in graphene. In this case, the RG equations lead to various nontrivial fixed points [32].

In conclusion, we have investigated the effects of magnetic impurities on the surface states of a TI. A magnetic impurity breaks TR symmetry and suppresses the low-energy LDOS locally. The surface states mediate a coupling between the magnetic impurities which is always ferromagnetic when the chemical potential lies close to the Dirac point. Therefore, we expect that a finite concentration of magnetic impurities would give rise to a ferromagnetic ground state on the surface. This mechanism provides a physical realization of the novel topological magnetoelectric effect discussed in Ref. [8], which requires breaking of TR symmetry on the surface of a TI. We also investigated the effect of quenched impurities on the surface states and presented the RG equations governing the flow of the coupling constants. We would like to emphasize that the effects we proposed in this Letter are unique for the surface of strong topological insulators. For a "weak" topological insulator [5–7] with even number of Dirac cones on the surface, the intercone scattering can change both the surface DOS distribution and the RKKY interaction between two magnetic impurities. The distinct signatures of magnetic impurities on the surface states of a TI discussed in this work can be readily observed in STM experiments, possibly on the surface of Be_2Se_3 and related TIs [14,15,33].

The authors would like to thank T. L. Hughes, J. Maciejko, T. X. Ma, S. Raghu, S. Ryu, and B. F. Zhu for helpful discussions. This work is supported by the U.S. Department of Energy, Office of Basic Energy Sciences under Contract DE-AC03-76SF00515. We also acknowledge financial support from the Focus Center Research Program (FCRP) Center on Functional Engineered Nanoarchitectonics (FENA). C. X. L. acknowledges CSC, NSF (Grant No. 10774086, 10574076) and Basic Research Development of China (Grant No. 2006CB921500).

[1] C. L. Kane *et al.*, Phys. Rev. Lett. **95**, 226801 (2005).
[2] B. A. Bernevig *et al.*, Phys. Rev. Lett. **96**, 106802 (2006).
[3] B. A. Bernevig *et al.*, Science **314**, 1757 (2006).
[4] M. Konig *et al.*, Science **318**, 766 (2007).
[5] L. Fu *et al.*, Phys. Rev. Lett. **98**, 106803 (2007).
[6] J. E. Moore *et al.*, Phys. Rev. B **75**, 121306(R) (2007).
[7] R. Roy *et al.*, arXiv:cond-mat/0607531.
[8] X.-L. Qi *et al.*, Phys. Rev. B **78**, 195424 (2008).
[9] C. Wu *et al.*, Phys. Rev. Lett. **96**, 106401 (2006).
[10] C. Xu *et al.*, Phys. Rev. B **73**, 045322 (2006).
[11] G. W. Semenoff, Phys. Rev. Lett. **53**, 2449 (1984).
[12] K. S. Novoselov *et al.*, Nature (London) **438**, 197 (2005).
[13] X.-L. Qi *et al.*, Nature Phys. **4**, 273 (2008).
[14] H. Zhang *et al.*, arXiv:0812.1622.
[15] Y. Xia *et al.*, arXiv:0812.2078.
[16] J. S. Dyck *et al.*, Phys. Rev. B **65**, 115212 (2002).
[17] Z. Zhou *et al.*, Appl. Phys. Lett. **87**, 112503 (2005).
[18] A. Matulis *et al.*, Phys. Rev. B **77**, 115423 (2008).
[19] T. O. Wehling *et al.*, Phys. Rev. B **75**, 125425 (2007).
[20] F. Meier *et al.*, Science **320**, 82 (2008).
[21] H. Shiba, Prog. Theor. Phys. **40**, 435 (1968).
[22] Z. F. Wang *et al.*, Phys. Rev. B **74**, 125417 (2006).
[23] L. Brey *et al.*, Phys. Rev. Lett. **99**, 116802 (2007).
[24] S. Saremi, Phys. Rev. B **76**, 184430 (2007).
[25] T. Jungwirth *et al.*, Rev. Mod. Phys. **78**, 809 (2006).
[26] E. Fradkin *et al.*, Phys. Rev. Lett. **57**, 2967 (1986).
[27] K. Nomura *et al.*, Phys. Rev. Lett. **100**, 246806 (2008).
[28] A. W. Ludwig *et al.*, Phys. Rev. B **50**, 7526 (1994).
[29] T. Stauber *et al.*, Phys. Rev. B **71**, 041406(R) (2005).
[30] O. Vafek *et al.*, Phys. Rev. B **77**, 033410 (2008).
[31] I. F. Herbut *et al.*, Phys. Rev. Lett. **100**, 046403 (2008).
[32] M. S. Foster *et al.*, Phys. Rev. B **77**, 195413 (2008).
[33] S. Urazhdin *et al.*, Phys. Rev. B **69**, 085313 (2004).